Published in final edited form as:
Angew Chem Int Ed Engl. 2014 July 14; 53(29): 7531–7534. doi:10.1002/anie.201403890.

Ultrafluorogenic Coumarin-Tetrazine Probes for Real-Time Biological Imaging**

Labros G. Meimetis[+], **Jonathan C.T. Carlson**[+], **Randy J. Giedt**, **Rainer H. Kohler**, and **Ralph Weissleder**

Center for Systems Biology, Massachusetts General Hospital 185 Cambridge Street, Boston, MA 02114 (USA)

Ralph Weissleder: rweissleder@mgh.harvard.edu

Abstract

We have developed a series of new ultrafluorogenic probes in the blue-green spectrum that display fluorescence enhancement exceeding 11,000-fold. These fluorogenic dyes integrate a coumarin fluorochrome with the bioorthogonal tetrazine-*trans*cyclooctene (TCO) chemistry platform. By exploiting highly efficient through bond energy transfer (TBET), these probes exhibit the highest brightness enhancements reported thus far for any bioorthogonal fluorogenic dyes. No-wash, fluorogenic imaging of diverse targets including cell surface receptors in cancer cells, mitochondria, and the actin cytoskeleton is possible within seconds with minimal background signal and no appreciable non-specific binding, opening the possibility for *in vivo* sensing.

Keywords

click chemistry; energy transfer; fluorescence probes; fluorogenic probes; tetrazines

One of the major challenges in clinical medicine and biomedical research remains accurate detection of abnormal cellular and subcellular events. This is particularly important in the detection of rare cancer cells in a sea of normal host cells[1], for improved diagnostic performance in point-of care devices[2], in detecting invading tumor margins during surgery[3], in determining drug effects at the single cell level[4] or for the detection of aberrant proteins. There have been tremendous advances in the development of optical sensing approaches but what is still generally lacking are efficient, cell permeable and and biocompatible fluorochromes with zero background. With most diagnostic read-outs (e.g. cytopathology, flow cytometry, microscopy) the background of fluorochrome-tagged affinity ligands is always a concern, necessitating careful optimization of staining conditions and extensive wash-steps. While this is feasible in larger sample sizes, where washing steps

**Part of this work was supported by National Institutes of Health grant number R01EB01011. We thank Dr. Katy Yang for cell culture assistance and Alex Zaltsman for microscopy assistance.

Correspondence to: Ralph Weissleder, rweissleder@mgh.harvard.edu.

[+]These authors contributed equally to this work.

Supporting information for this article is available on the WWW under http://dx.doi.org/10.1002/anie.201xxxxxx.

are well tolerated, it becomes much more difficult with scant cell populations (e.g. circulating tumor cells, stem cells, immune cell subtypes), in microfluidic point-of-care devices where wash steps are more difficult to incorporate, and in the labeling of small molecules, whose properties are frequently perturbed by fluorescent tags. For these reasons, new fluorochromes with zero background but extensive bioorthogonal amplification are needed.

Pioneering work has built probes around the Staudinger ligation and azide-alkyne cycloaddition “click” platforms that have principally employed photoinduced electron transfer (PET) or Förster resonance energy transfer (FRET) as a mechanism of suppressing fluorescence emission.[5] Unfortunately, in spite of laborious design efforts to customize quenching mechanisms for a given fluorophore system, the modest brightness enhancement of these probes (typically < 30-fold) yields relatively poor target-to-background ratios and thus limits their utility *in vivo*. More recently, we reported on BODIPY-tetrazine conjugates that achieved higher amplifications (up to 1600-fold) in the green spectrum via through bond energy transfer (TBET).[6] By providing a conduit for energy transfer within a contiguous scaffold of pi bonds, TBET circumvents many of the solvent, spatial, and spectral limitations that PET and FRET exhibit and can yield very high efficiencies.[7] However, multicolor TBET probes have not been synthesized to date. Eager to extend the current armamentarium of cell permeable and biocompatible ultrafluorogenic probes, we set out to systematically develop a series of bioorthogonal probes in the blue-green spectrum (**H**yper**E**missive **L**igation-**I**nitiated **O**rthogonal **S**ensing, HELIOS probes). Here we report a series of such molecules with the highest turn-on ratios to date.

Coumarin fluorochromes are small, biocompatible, and widely used for *in vivo* and *in vitro* diagnostics and imaging.[8] They encompass an extensive spectral range, with the brightest fluorochromes exciting and emitting in the blue spectral region. We selected coumarin 102 (**1**) (Scheme 1) as a starting point. It has a high quantum yield in water (phi = 0.66),[9] a peak absorbance compatible with 405nm laser excitation, and a previously described transition dipole,[10] relevant to rational probe design. Energy transfer and fluorogenic switching should be maximized by collinear alignment of the emission transition dipole of coumarin 102 with the absorption transition dipole of tetrazine, which is perpendicular to the heterocyclic plane (Figure 1a).[11]

Although several synthetic approaches are possible we postulated that appending a phenyl tetrazine at the C3 position of **1** would allow for efficient TBET, and that the *meta* configuration would yield maximum fluorescence attenuation. To this end, we brominated **1** with *N*-Bromosuccinimide, followed by a Suzuki coupling with 3-cyanophenylboronic acid and catalytic $Pd(OAc)_2(PPh_3)_2$ in refluxing dioxane/water (see supplementary information). The resultant nitrile in dioxane was treated with hydrazine, $Zn(OTf)_2$, and acetonitrile then heated to 60 °C.[12] Treatment of the crude mixture with sodium nitrite, followed by an acidic workup furnished the corresponding methyltetrazine Helios 400Me in three steps from commercially available materials (Scheme 1). To serve as a mechanistic control, we constructed the *para*-substituted tetrazine analogue HELIOS 400*p*Me by a parallel route (see the Supporting Information). The transition dipoles between donor and acceptor of this probe are nearly perpendicular and would thus be predicted to yield negligible quenching by

FRET (Figure 1a). As such, measuring the turn-on relative to the meta-substituted HELIOS 400Me provides a facile method to validate TBET as the underlying mechanism for fluorescence quenching.

HELIOS 400Me and HELIOS 400pMe were both soluble in phosphate buffered saline (PBS) at micromolar concentrations and negligibly fluorescent in their native state. After rigorous purification to remove trace fluorescent impurities, we evaluated the fluorogenic properties of these new coumarin-Tz conjugates on reaction with TCOc, a novel trans-cyclooctene derivative (TCOc) that incorporates a carbamate-linked PEG_2 side chain for improved water solubility (see the Supporting Information). Addition of TCOc to HELIOS 400Me in PBS yielded a 4,000-fold peak turn-on ratio (Figure 1b). Reaction of HELIOS 400*p*Me with TCOc yielded a turn on ratio of 1,000-fold, four-fold lower than its *meta*-linked counterpart. Mechanistically, the observation of 1000-fold turn-on in a perpendicular-dipole configuration argues against FRET playing a significant role in the energy transfer mechanism.[13] Furthermore, the fluorescence emission intensity of the native probes was found to be independent of solvent polarity, which suggests that PET is not the operative photophysical quenching mechanism for these probes (Figure S1, Supporting Information).

Encouraged by this outcome, we next implemented this design in a series of structurally diverse coumarins that span the full blue spectral range (Figure 2a). We again selected dyes known to retain bright fluorescence emission in aqueous solution, including Coumarin 339 (**2**),[14] Coumarin 120 (**3**), and difluorinated hydroxycoumarin **4**[15](Scheme 1). The same modular synthetic approach of bromination, Suzuki coupling, followed by metal-catalyzed tetrazine formation was used to generate this small library of coumarin-Tz conjugates (Scheme 1). HELIOS 388Me in PBS yielded a remarkable 11,000-fold turn-on upon reaction with TCOc, the highest turn-on ratio reported to date. When ligated to TCOc in PBS, HELIOS 347Me and HELIOS 370Me displayed 2,500-fold and 2,900-fold turn-on ratios, respectively, in spite of minimal spectral overlap with the tetrazine absorption band at 520nm. By comparison, FRET-based coumarin-tetrazine interactions are dramatically less efficient: a flexibly linked analogue of HELIOS 370H displayed only a 60-fold turn-on (Marina Blue-Tz, see the Supporting Information), corroborating the dipole-orientation analysis above. All four HELIOS probes exhibit very good post-click quantum yields in PBS, in agreement with structurally similar coumarins (Table 1).

To demonstrate the applicability of these probes as native bioorthogonal fluorogenic imaging agents, we used HELIOS 370H. We chose a simple model system to assess HELIOS probe kinetics in the extracellular context: imaging of the epidermal growth factor receptor (EGFR) on the surface of cancer cells. EGFR overexpression plays a critical role in the most common molecularly-defined subtype of lung cancer, where it is a key treatment target, and drives proliferation in other epithelial malignancies, including colon cancer and pancreatic cancer.[16] A431 cells were incubated with a TCO labeled anti-EGFR antibody (20μg/mL, Cetuximab, ImClone) for 20 minutes and then washed briefly with PBS. Addition of 100nM HELIOS 370H in PBS revealed bright, membrane specific staining coinciding with the known distribution of the receptor (Figure 2c). Images were generated within seconds of dye addition and exhibited no nonspecific binding even after extended

incubation, nor any membrane staining in the presence of a control antibody-TCO conjugate (see the Supporting Information).

To further explore the imaging potential of HELIOS probes, we selected mitochondria as a target; their structures have features at the diffraction limit of conventional light microscopy. OVCA-429 cells expressing mitochondria-specific red fluorescent protein (RFP) were incubated with an anti-mitochondria antibody-TCO conjugate and visualized with HELIOS 388H, yielding high spatial resolution images with good colocalization (Figure 3a). Intracellular imaging of small molecule targets is another area of intense interest, given the potential applications in drug development, chemical biology, and optical pharmacology. To demonstrate the utility of HELIOS probes in this context with a structurally validated model system, we tested their ability to image the actin cytoskeleton with a phalloidin-TCO conjugate (see the Supporting Information). Sequential addition of phalloidin-TCO and several HELIOS probes produced vivid fluorogenic images of the cytoskeleton; control experiments revealed negligible background (Figure 3b).

In summary, the library of turn-on HELIOS probes spans the visible spectrum from blue to green, providing appealing optical flexibility for imaging applications and validating the generality and robustness of the TBET-tetrazine mechanism. The fast, catalyst-free, and exceptionally fluorogenic reactivity of these probes should synergize with emerging methods for facile dienophile labelling of biological targets, including metabolically incorporated cyclopropenes[17] and TCO-amino acids.[18] We believe this series of HELIOS dyes will prove useful *in vitro*, *in vivo*, and in diagnostic settings, in addition to enhancing methods for super-resolution microscopy.

Supplementary Material

Refer to Web version on PubMed Central for supplementary material.

References

1. Ullal AV, Peterson V, Agasti SS, Tuang S, Juric D, Castro CM, Weissleder R. Sci. Transl. Med. 2014; 6 219ra9.
2. Peterson VM, Castro CM, Chung J, Miller NC, Ullal AV, Castano MD, Penson RT, Lee H, Birrer MJ, Weissleder R. Proc. Natl. Acad. Sci. U. S. A. 2013; 110:E4978. [PubMed: 24297935]
3. van Dam GM, et al. Nat. Med. 2011; 17:1315. [PubMed: 21926976]
4. Thurber GM, Yang KS, Reiner T, Kohler RH, Sorger P, Mitchison T, Weissleder R. Nat. Commun. 2013; 4:1504. [PubMed: 23422672]
5. Sivakumar K, Xie F, Cash BM, Long S, Barnhill HN, Wang Q. Org. Lett. 2004; 6:4603. [PubMed: 15548086] Devaraj NK, Hilderbrand S, Upadhyay R, Mazitschek R, Weissleder R. Angew. Chem. Int. Ed. 2010; 49:2869.Angew. Chem. 2010; 122:2931.Jewett JC, Bertozzi CR. Org. Lett. 2011; 13:5937. [PubMed: 22029411] Shieh P, Hangauer MJ, Bertozzi CR. J. Am. Chem. Soc. 2012; 134:17428. [PubMed: 23025473]
6. Carlson JCT, Meimetis LG, Hilderbrand SA, Weissleder R. Angew. Chem. Int. Ed. 2013; 52:6917.Angew. Chem. 2013; 125:7055.
7. Speiser S. Chem. Rev. 1996; 96:1953. [PubMed: 11848817]
8. Uttamapinant C, White KA, Baruah H, Thompson S, Fernández-Suárez M, Puthenveetil S, Ting AY. Proc. Natl. Acad. Sci. U. S. A. 2010; 107:10914. [PubMed: 20534555] Signore G, Nifosì R, Albertazzi L, Storti B, Bizzarri R. J. Am. Chem. Soc. 2010; 132:1276. [PubMed: 20050646]

9. Jones G, Jackson WR, Choi CY, Bergmark WR. J. Phys. Chem. 1985; 89:294.
10. Theisen M, Linke M, Kerbs M, Fidder H, Madjet ME-A, Zacarias A, Heyne K. J. Chem. Phys. 2009; 131:124511. [PubMed: 19791898]
11. Kim TG, Castro JC, Loudet A, Jiao JG-S, Hochstrasser RM, Burgess K, Topp MR. J. Phys. Chem. A. 2006; 110:20. [PubMed: 16392835]
12. Yang JJ, Karver MR, Li WW, Sahu SS, Devaraj NK. Angew. Chem. Int. Ed. 2012; 51:5222.Angew. Chem. 2012; 124:5312–5315.
13. Giribabu L, Ashok Kumar A, Neeraja V, Maiya BG. Angew. Chem. Int. Ed. 2001; 40:3621.Angew. Chem. 2001; 113:3733–3736.Lakowicz, JR. Principles of Fluorescence Spectroscopy. Springer; 2009. p. 954
14. Atkins RL, Bliss DE. J. Org. Chem. 1978; 43:1975.
15. Hedberg C, Dekker FJ, Rusch M, Renner S, Wetzel S, Vartak N, Gerding-Reimers C, Bon RS, Bastiaens PIH, Waldmann H. Angew. Chem. Int. Ed. 2011; 50:9832.Angew. Chem. 2011; 123:10006.
16. Ciardiello F, Tortora G. N. Engl. J. Med. 2008; 358:1160. [PubMed: 18337605]
17. Cole CM, Yang J, Šečkutė J, Devaraj NK. Chembiochem. 2013; 14:205. [PubMed: 23292753] Patterson DM, Nazarova LA, Xie B, Kamber DN, Prescher JA. J. Am. Chem. Soc. 2012; 134:18638. [PubMed: 23072583] Yang J, Šečkutė J, Cole CM, Devaraj NK. Angew. Chem. Int. Ed. 2012; 51:7476.Angew. Chem. 2012; 124:7594–7597.
18. Nikić I, Plass T, Schraidt O, Szymański J, Briggs JAG, Schultz C, Lemke EA. Angew. Chem. Int. Ed. 2014; 53:2245.Angew. Chem. 2014; 126:2278–2282.

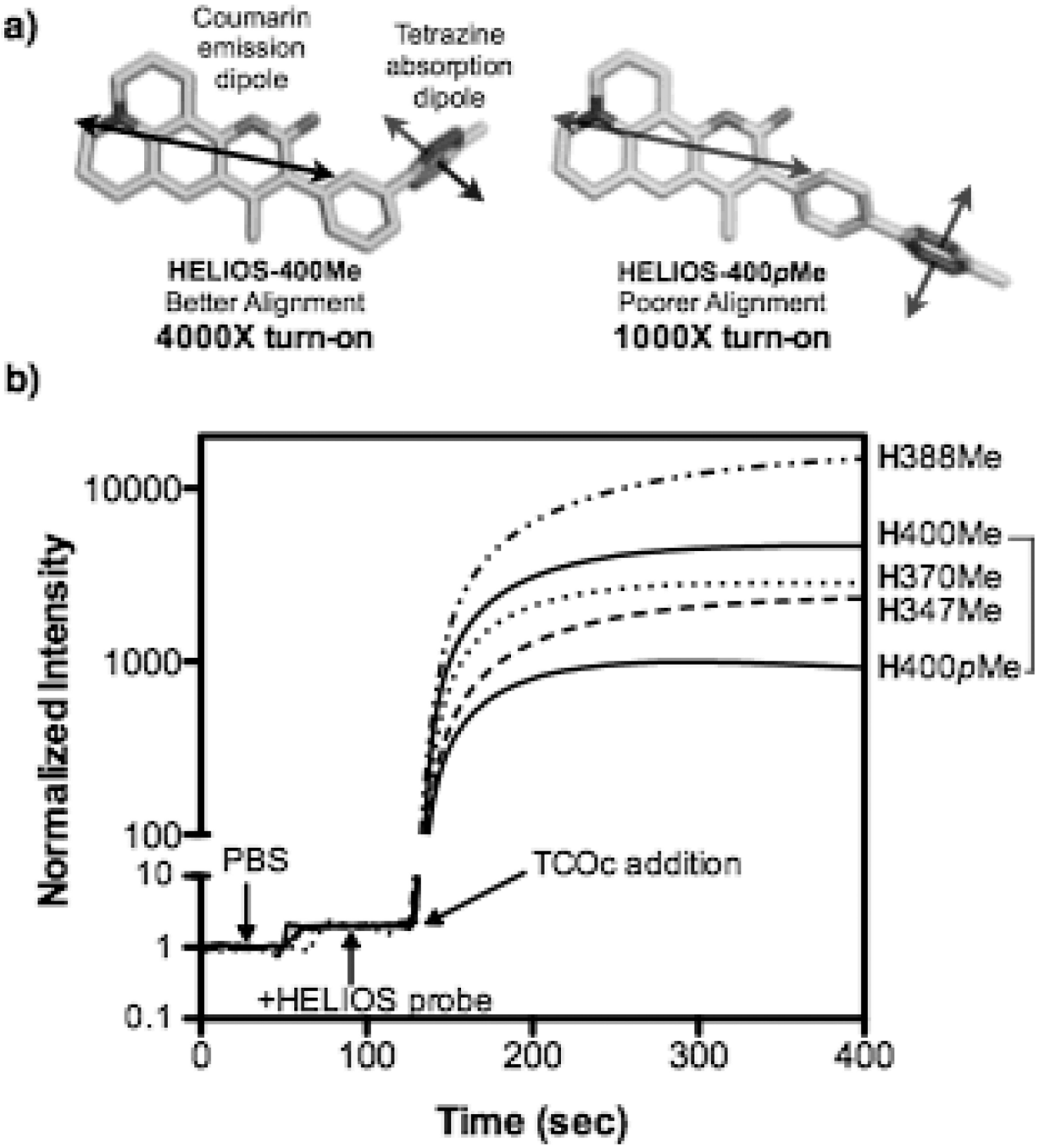

Figure 1.

a) Comparison of approximate transition dipole orientation between coumarin 102[10] and tetrazine[11] in HELIOS 400Me and HELIOS 400*p*Me. b) Fluorogenic activation timecourse of HELIOS probes upon reaction with TCOc (**H** = HELIOS).

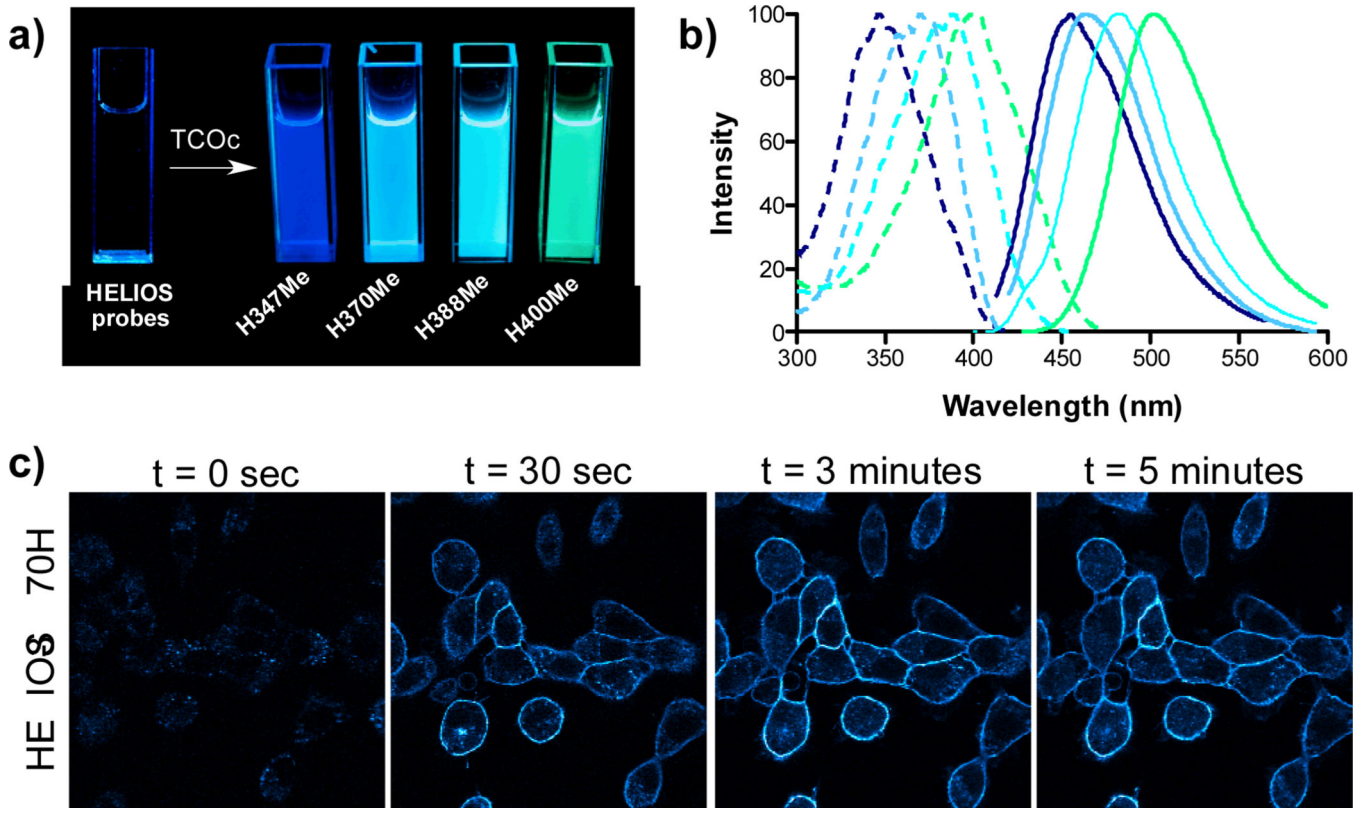

Figure 2.

a) Visualization of the turn-on response using a handheld UV lamp: On the left is a cuvette containing HELIOS 347Me in PBS. On the right are cuvettes with individual HELIOS probes + TCOc in PBS. b) Normalized absorption and emission spectra of clicked products in PBS. c) No wash fluorogenic imaging of EGFR expression on A431 cells. Cells were incubated with an α-EGFR–TCO antibody (0.2mcg/mL), washed briefly, and then imaged sequentially after addition of 100 nM HELIOS 370H in PBS. Bright, membrane-specific staining is visible within seconds, peaks within 3 minutes and is stable thereafter.

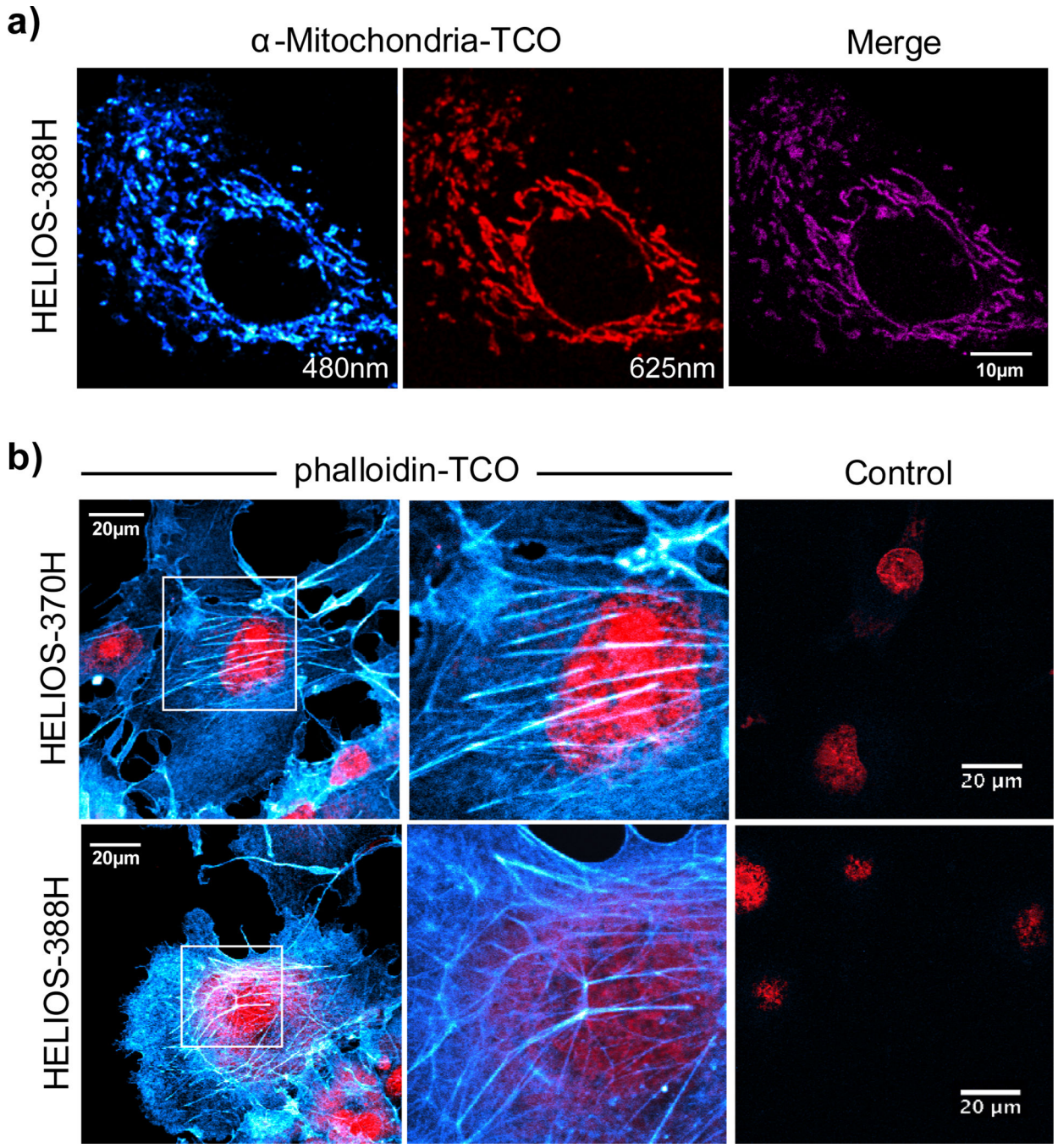

Figure 3. No-wash fluorogenic imaging of intracellular targets

a) Mitochondrial imaging: OVCA-429 cells with RFP-tagged mitochondria were incubated with an anti-mitochondria-TCO antibody, rinsed briefly, and then imaged after addition of 100nM HELIOS-388H in PBS. Colocalization analysis in ImageJ (Costes auto-threshold) was used to generate the merged image in the right-hand panel. b) Actin imaging: COS-1 cells were incubated with phalloidin-TCO (1μg/mL) and DRAQ5 nuclear counterstain (1μM, BioStatus), rinsed briefly, and then imaged upon addition of the indicated HELIOS

probe at 100nM. Control images were collected at matched dye concentrations in the absence of phalloidin-TCO.

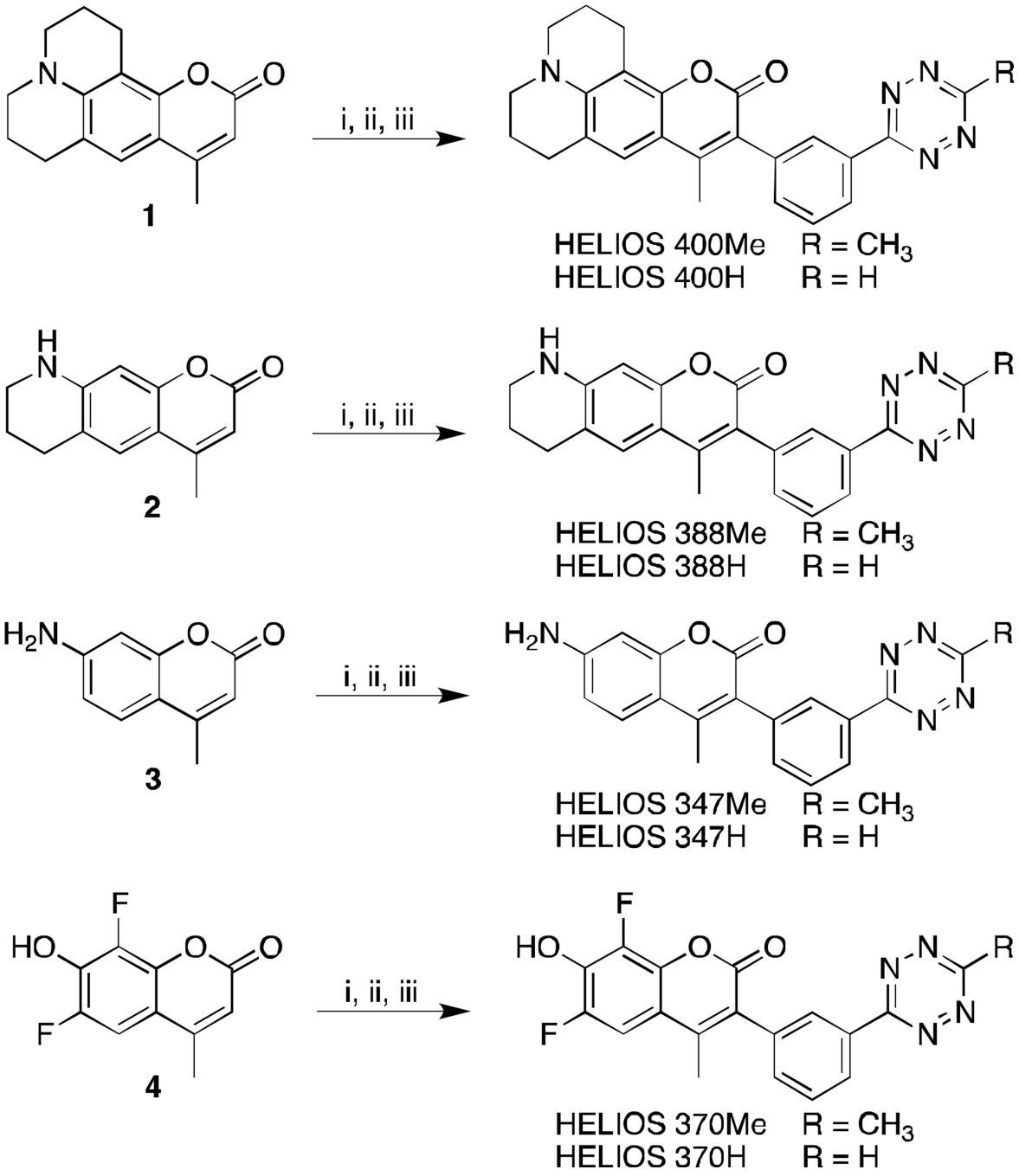

Scheme 1.

Synthetic scheme for bioorthogonal fluorogenic HELIOS probes. i) *N*-Bromosuccinimide in acetonitrile, ii) 3-cyanophenylboronic acid, $Pd(OAc)_2(PPh_3)_2$, K_2CO_3 in 75 % $dioxane_{(aq)}$ at 100 °C, iii) hydrazine, $Zn(OTf)_2$, acetonitrile/dioxane (Me-Tz) or formamidine hydrochloride/DMF (H-Tz) at 60 °C for 15h followed by $NaNO_2$ and HCl.

Table 1

Photophysical Properties

Probe	Peak Ex/Em Wavelengths	ε[a]	Φ w/TCOc[b]	Fluorescence Enhancement[c]
HELIOS 400	400/502	16,000	0.41	4,000-fold
HELIOS 388	388/482	20,000	0.38	11,000-fold
HELIOS 370	370/463	19,000	0.49	2,900-fold
HELIOS 347	347/455	18,500	0.29	2,500-fold
Marina Blue-Tz	362/459	ND	ND	60-fold

[a] At peak excitation wavelength in PBS, pH 7.4.

[b] Quantum yield for the dihydropyridazine product after complete reaction of the indicated compound with TCOc in PBS at pH 7.4; quinine sulfate in H_2SO_4 (0.5M, $\Phi = 0.546$) was used as the standard.

[c] Fluorogenic turn-on ratio of the Me-tetrazines upon reaction with TCOc.